Hindawi
Mathematical Problems in Engineering
Volume 2017, Article ID 6504969, 13 pages
https://doi.org/10.1155/2017/6504969

Research Article

Coexisting Oscillation and Extreme Multistability for a Memcapacitor-Based Circuit

Guangyi Wang,[1] Chuanbao Shi,[1] Xiaowei Wang,[2] and Fang Yuan[1]

[1]*Institute of Modern Circuits and Intelligent Information, Hangzhou Dianzi University, Hangzhou 310018, China*
[2]*Department of Automation, Shanghai University, Shanghai 200072, China*

Correspondence should be addressed to Xiaowei Wang; laura423_wang@163.com

Received 6 September 2016; Revised 7 November 2016; Accepted 6 December 2016; Published 23 January 2017

Academic Editor: Mingshu Peng

The coexisting oscillations are observed with a memcapacitor-based circuit that consists of two linear inductors, two linear resistors, and an active nonlinear charge-controlled memcapacitor. We analyze the dynamics of this circuit and find that it owns an infinite number of equilibrium points and coexisting attractors, which means extreme multistability arises. Furthermore, we also show the stability of the infinite many equilibria and analyze the coexistence of fix point, limit cycle, and chaotic attractor in detail. Finally, an experimental result of the proposed oscillator via an analog electronic circuit is given.

1. Introduction

Memristor is known as the fourth basic circuit element that was firstly postulated by Chua in 1971 [1] and has attracted worldwide immense attention from both theory and applications even since a solid-state device called the memristor was fabricated by the HP Lab in 2008 [2]. Then, Di Ventra et al. extend the notion of memristor to memcapacitor and meminductor [3], whose properties depend on the state and history of them in circuit. These nanoscale elements, that store information without need for an internal power supply, can be used for nonvolatile memories, nonlinear circuits, neural networks, and so on.

In the field of nonlinear dynamics, memristors can be as fundamental elements for the designs of new nonlinear circuits substituting other nonlinear devices, whereupon many memristor-based chaotic oscillators were presented by using HP memristor and the other memristor models of piecewise linear, quadric, and cubic φ-q (flux-charge) functions. Itoh and Chua firstly derived several nonlinear oscillators based on Chua's oscillators by replacing Chua's diodes with piecewise linear models of memristor [4]. The authors in [5] designed a periodically forced memristive Chua's circuit using the flux-controlled memductance model $W(\varphi) = -a + b|\varphi(t)|$. HP memristor model is a first model of actual memristive device, which was implemented by a memristor emulator in [6]. The paper [7] introduced a complete mathematical model for the HP memristor which takes into consideration all boundary situations providing the interrelation between memristance charge and flux. Based on HP memristor and other memristor models, some chaotic oscillators were presented [8–10]. Recently, a new memristor-based chaotic system was designed based on HP memristor in [11] and was realized using FPGA (Field Programmable Gate Array) technology. A novel digital-analog hybrid chaotic system with generalized memristor was constructed for the production of random number [12]. However, the memcapacitor and meminductor have received a little attention since the actual solid-state devices of them have not been successfully achieved. Because of their potential application values, memcapacitor and meminductor have still attracted more and more attentions.

The first meminductor emulator was designed in [13] whose inductance can be varied by an external current source without employing any memristive system. In [14], a flux-controlled memristive emulator using light-dependent resistor (LDR) was proposed and the mutator for transferring memristor into a flux-controlled meminductor is described.

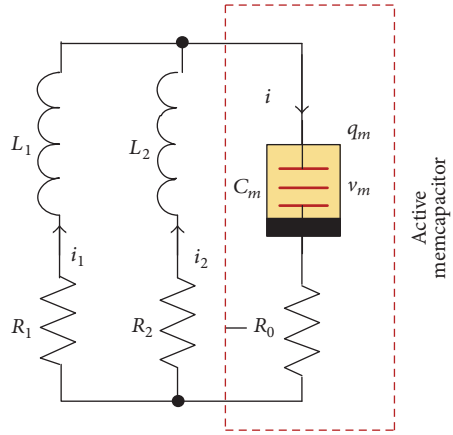

Figure 1: Memcapacitor-based circuit.

A mathematical model of a flux-controlled meminductor and its equivalent circuit model for exploring the properties of the meminductor in a nonlinear circuit were presented in [15].

It would be worthwhile to prospectively study effective memcapacitor models and its applications. So several memcapacitor models, including piecewise linear, quadric and cubic function models, memristor-based memcapacitor models, and memcapacitor emulators, were proposed in [16–21], and a mathematical memcapacitor model and a corresponding circuit model are established in [22]. Some special phenomena such as hidden attractors, coexistence attractors, and extreme multistability were found in memcapacitor-based chaotic oscillators [23, 24] and memristor-based chaotic oscillators [25–27]. In fact, multistability and coexisting attractors have caught the attention of researcher in general chaotic systems [28–30].

This paper introduces a new chaotic oscillator based on a charge-controlled memcapacitor model and its dynamical behaviors are analyzed. The most important properties of the memcapacitor-based circuit are that it possesses an infinite number of equilibrium points and coexisting attractors and displays the coexisting attractors and stability of the infinite many equilibria, called extreme multistability. The rest of this paper is organized as follows. In Section 2, the chaotic oscillator is described and the typical chaotic attractors are given. In Section 3, the dissipativity and equilibrium stability of the system are studied. In Section 4, coexisting attractors with different initial $x(0)$ and $u(0)$ are described. In Section 5, an analog circuit is designed to realize the memcapacitor-based oscillator. Finally, some conclusions of this paper are given in Section 6.

2. Memcapacitor-Based Chaotic Oscillator Circuit

The chaotic oscillator circuit based on a charge-controlled memcapacitor is shown in Figure 1, which contains two linear inductors, L_1 and L_2, two linear resistors, R_1 and R_2, and an active memcapacitor. The active memcapacitor is an active 2-terminal circuit consisting of a linear active resistor $-R_0$ and a nonlinear memcapacitor in series, in which the active resistor $-R_0$ provides energy for the circuit. Hence, the series circuit, that is, the active 2-terminal circuit as a whole, exhibits an active feature, so called the active memcapacitor.

Table 1: Parameters of system (3).

Parameter	Value
$a = \alpha/L_1$	5.8
$b = \beta/L_1$	1.5
$c = (R_0 - R_1)/L_1$	2.6
$d = R_0/L_1$	0.1
$e = (R_0 - R_2)/L_2$	−3.4
$f = R_0/L_2$	0.2
$m = \beta/L_2$	6.8
$n = \alpha/L_2$	2.8

The circuit dynamics can be described by

$$\begin{aligned} L_1\frac{di_1}{dt} &= (i_1 + i_2)R_0 - v_m - i_1R_1, \\ L_2\frac{di_2}{dt} &= (i_1 + i_2)R_0 - v_m - i_2R_2, \\ \frac{dq_m}{dt} &= i_1 + i_2, \end{aligned} \tag{1}$$

where q_m and v_m are the charge through the memcapacitor and the voltage across the memcapacitor, respectively. The relationship between the charge q_m and voltage v_m of the memcapacitor is defined as [19]

$$v_m = \left(\alpha + \beta\sigma_m^2\right)q_m, \tag{2}$$

where $\alpha + \beta\sigma_m^2$ is the inverse memcapacitance and σ_m is the time integral of q_m; namely, $\sigma = \int_{t_0}^{t} q(\tau)d\tau$.

Equation (2) has a new variable σ_m, so we should add an equation of σ_m in (1). If we define $x = i_1$, $y = i_2$, $z = q_m$, $u = \sigma_m$, $a = \alpha/L_1$, $b = \beta/L_1$, $c = (R_0 - R_1)/L_1$, $d = R_0/L_1$, $e = (R_0 - R_2)/L_2$, $f = R_0/L_2$, $m = \beta/L_2$, and $n = \alpha/L_2$, (1) becomes

$$\begin{aligned} \frac{dx}{dt} &= cx + dy - az - bzu^2, \\ \frac{dy}{dt} &= fx + ey - nz - mzu^2, \\ \frac{dz}{dt} &= x + y, \\ \frac{du}{dt} &= z. \end{aligned} \tag{3}$$

Typical chaotic attractors obtained by simulating (3) are shown in Figure 2 in terms of the parameters listed in Table 1, with the initial condition (0.01, 0.01, 0.01, 0.01).

The corresponding Lyapunov exponents are calculated as $\mathrm{LE}_1 = 0.3787$, $\mathrm{LE}_2 = 0.0092$, $\mathrm{LE}_3 = -0.0094$, and $\mathrm{LE}_4 = -0.9786$. The Poincare mapping on $z = 0$ and the time-domain waveforms of system (3) are described in Figure 3.

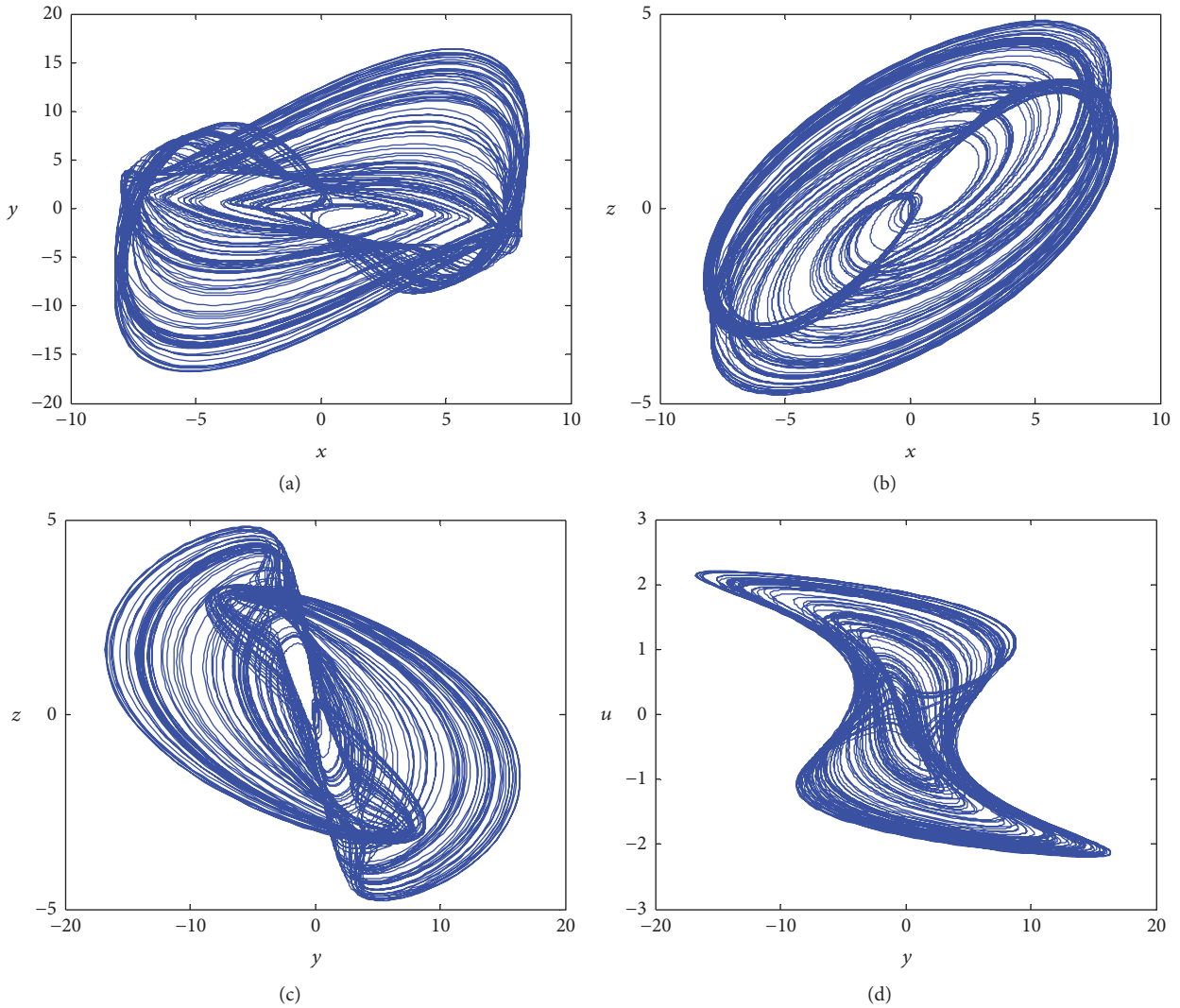

Figure 2: Chaotic attractors obtained from (3). (a) x-y plane. (b) x-z plane. (c) y-z plane. (d) y-u plane.

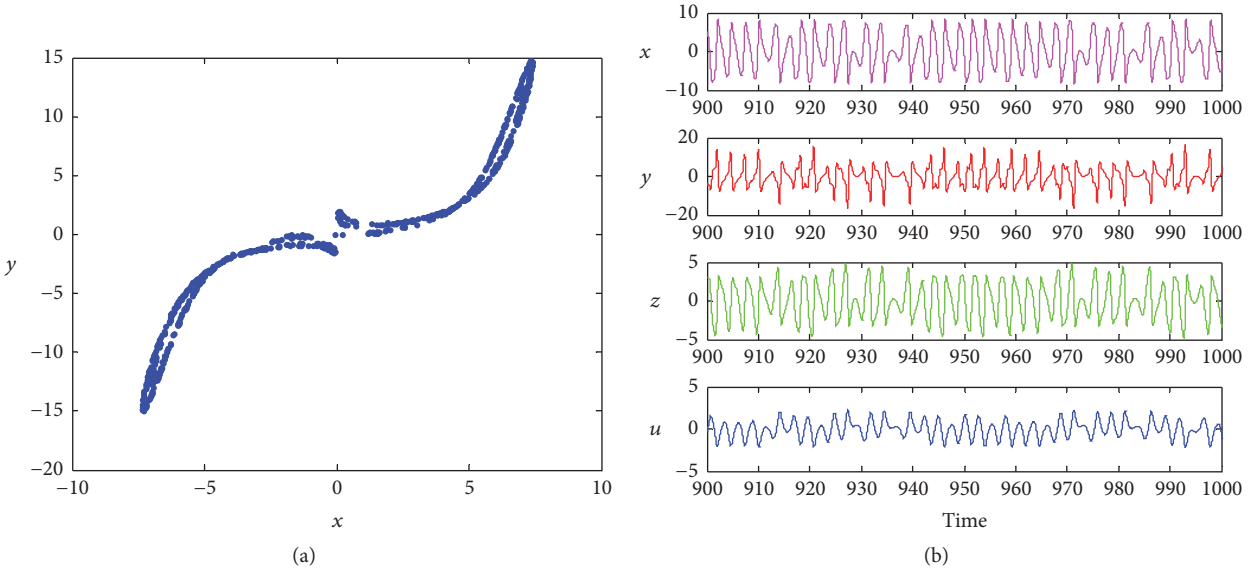

Figure 3: Poincare mapping and time-domain waveforms. (a) Poincare mapping. (b) Time-domain waveforms.

Obviously, time-domain waveforms are nonperiodic continuous chaotic sequences, and the curve of Poincare map is a continuous curve, and the time-domain waveform is not periodic, which indicate that these attractors are chaotic attractors.

3. Dynamical Characteristic Analysis

3.1. Dissipativity and Stability of Equilibrium Set. Dissipative systems will shrink to a phase space of a limited area, called the attractor. The dissipativity of the system is described as

$$\nabla V = \frac{\partial \dot{x}}{\partial x} + \frac{\partial \dot{y}}{\partial y} + \frac{\partial \dot{z}}{\partial z} + \frac{\partial \dot{u}}{\partial u} = c + e. \tag{4}$$

When the parameters are set as $c = 2.6$ and $e = -3.4$, the exponential constraint rate satisfies

$$\nabla V = -0.8 < 0. \tag{5}$$

It means that the volume of phase space will be contracted to zero and all trajectories of the system are confined to a subset of zero volume.

The equilibrium points of system (3) can be calculated as

$$\begin{aligned} s_1 &= \{(x, y, z, u) \mid z = 0, x = k_1, y = -k_1, u = k_2\}, \\ &\qquad\qquad c = d,\ f = e, \\ s_2 &= \{(x, y, z, u) \mid x = y = z = 0, u = k_3\}, \\ &\qquad\qquad c \neq d,\ f \neq e, \end{aligned} \tag{6}$$

where k_1, k_2, and k_3 are arbitrary constants. Obviously, the system has two equilibrium sets, and every set has an infinite number of equilibria.

If the parameters are $c = d$, $f = e$ or $c \neq d$, $f \neq e$, the Jacobian matrix of the circuit at equilibrium sets S_1 and S_2 is given by

$$J_{1,2} = \begin{bmatrix} c & d & -a - bk_{2,3}^2 & 0 \\ f & e & -n - mk_{2,3}^2 & 0 \\ 1 & 1 & 0 & 0 \\ 0 & 0 & 1 & 0 \end{bmatrix}, \tag{7}$$

where k_2 and k_3 have the same effect on the system, so they can be replaced by k. The characteristic equation is written as

$$\begin{aligned} &\lambda^4 - (c + e)\lambda^3 + \left(a + bk^2 + n + mk^2 + ce - fd\right)\lambda^2 \\ &\quad + \left(af + bk^2 f + dn + dmk^2 - ae - bk^2 e - nc \right. \\ &\quad \left. - cmk^2\right)\lambda = 0. \end{aligned} \tag{8}$$

According to the Routh–Hurwitz criterion, the necessary and sufficient condition for stability of the system is that all the principal minors are greater than zero; that is,

$$\begin{aligned} \Delta_1 &= a_1 > 0, \\ \Delta_2 &= \begin{vmatrix} a_1 & a_0 \\ a_3 & a_2 \end{vmatrix} > 0, \\ \Delta_3 &= \begin{vmatrix} a_1 & a_0 & 0 \\ a_3 & a_2 & a_1 \\ 0 & a_4 & a_3 \end{vmatrix} > 0, \\ \Delta_4 &= \begin{vmatrix} a_1 & a_0 & 0 & 0 \\ a_3 & a_2 & a_1 & a_0 \\ 0 & a_4 & a_3 & a_2 \\ 0 & 0 & 0 & a_4 \end{vmatrix} > 0, \end{aligned} \tag{9}$$

where

$$\begin{aligned} a_0 &= 1, \\ a_1 &= -(c + e), \\ a_2 &= a + bk^2 + n + mk^2 + ce - fd, \\ a_3 &= af + bk^2 f + dn + dmk^2 - ae - bk^2 e - nc \\ &\quad - cmk^2, \\ a_4 &= 0, \end{aligned} \tag{10}$$

whereas it is unstable and has the possibility of generating chaos under the proper parameters. If we fix $a = 5.8$, $b = 1.5$, $c = 2.6$, $d = 0.1$, $e = -3.4$, $f = 0.2$, $m = 6.8$, and $n = 2.8$, the stability of equilibrium sets S_1 and S_2 depends on the constant k. Figure 4 shows the change rule of Δ_1, Δ_2, Δ_3, and Δ_4 with the constant k. Here, Δ_1 is slightly greater than zero and Δ_4 is equal to zero, so the black curve overlaps so much with the green curve in Figure 4. Note that the stability of an infinite number of equilibria is called extreme multistability. The following analysis will show that the stability of the all equilibrium points depends on the parameter k, resulting in chaos when $k \in [-1.5, 1.5]$.

3.2. Coexisting Oscillations. In this section, we show that the dynamics of the system depend on not only its parameters but also its initial conditions, which leads to a special characteristic, called the coexisting oscillation in this paper. In the coexisting oscillation, many coexisting attractors appear with different initial conditions, such as coexistence of limit circle or fixed point and chaotic attractor, coexistence of chaotic and hyperchaotic attractors, and coexistence of two limits or two fixed points.

Multistability is a common phenomenon in many nonlinear systems, which corresponds to the coexistence of more than one stable attractor for the same set of system parameters [31]. If infinitely many attractors coexist for the same set of system parameters, the phenomenon is called extreme

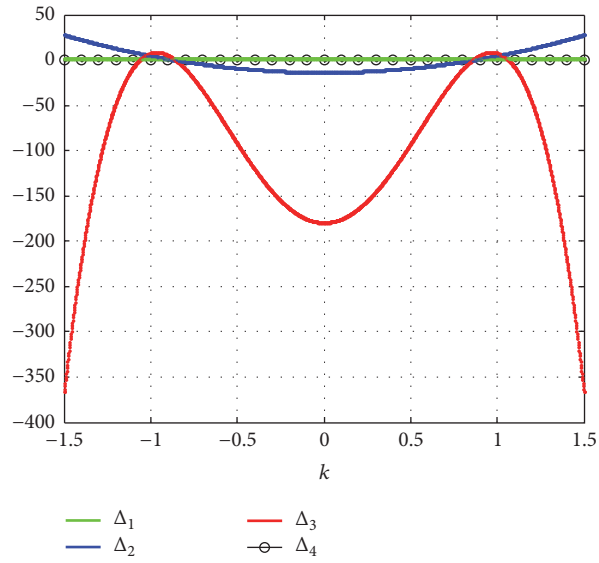

FIGURE 4: Curves of Δ_1, Δ_2, Δ_3, and Δ_4 with k.

multistability [32], showing that various coexisting attractors have essentially extreme multistability.

3.2.1. Coexisting Attractors with Initial Variable $x(0)$. If we fix the parameters as Table 1 and vary initial value $x(0)$ in the initial conditions (x_0, 0.01, 0.01, 0.01), the bifurcation diagram and corresponding Lyapunov exponent spectrum with respect to $x(0)$ can be obtained as shown in Figure 5. System (3), with the increase of initial state $x(0)$ in Figure 5, undergoes a complex bifurcation from chaos to period, or from period to chaos, implying the coexistence of periodic and chaotic attractors.

When $x(0)$ is varied, many coexisting attractors appear, as shown in Figure 6, in which every subdiagram represents a pair of coexisting attractors; the blue attractor and the red attractor start from different initial values of $x(0)$. The blue attractors start from $x(0) \in (-0.85, 0)$ and the red attractors start from $x(0) \in (0, 0.84)$. From Figure 6, we can see that there exist different coexistence attractors, including coexistence of a pair of chaotic attractors, coexistence of a pair of quasiperiodic limit cycles, and coexistence of a pair of limit cycles. Various coexisting attractors and their corresponding initial values are listed in Table 2.

3.2.2. Coexisting Attractors with Initial Variable $u(0)$. Similar to the abovementioned, the bifurcation diagrams and Lyapunov exponent spectrums with respect to the initial value $u(0)$ are described in Figure 7, in which we also fix parameters as Table 1 and vary parameter $u(0)$ in the initial condition: (0.01, 0.01, 0.01, u_0). Figures 7(a) and 7(b) indicate that the system undergoes a period-doubling bifurcation in the region $u(0) \in [-1, -0.65]$ and then enters chaos in the region $u(0) \in [-0.65, -0.59]$. With the further increase of $u(0)$, Figures 7(c) and 7(d) show that this system possesses the symmetric dynamics characteristic with respect to $u(0) = 1.05$ at the region $u(0) \in [0.6, 1.5]$.

Coexisting attractors with respect to initial value $u(0)$ are shown in Figure 8, and the corresponding regimes and initial conditions for all attractors are listed in Table 3. Note that Figure 8(a) shows the coexistence of the three attractors, that is, fixed point, two different limited circles.

Note that the phenomenon of coexisting oscillation is different with the initial value sensitivity of usual chaotic systems. For the usual chaotic system, trajectories starting from different initial values evolve along with the time and eventually converge to the same chaotic attractor. For the proposed oscillator, however, trajectories starting from different initial values can converge eventually to different attractors, including chaotic attractors, periodic attractors, or fixed points. Hence, it seems that trajectories in the coexisting attractors are more sensitive to initial values not only for chaotic orbits but also for periodic orbits.

4. Dimension Reduction Analysis

In order to solve the 3D equations (1), we must add an equation of σ_m which is an internal variable of the memcapacitor and obtain the 4D equations (3). However, this makes it difficult to solve the 4D equations. In general, if there is one memory element increased into a circuit, there will be two state equations added to the system equations, in which one is the equation corresponding to a circuit state variable and the other corresponds to the internal variable for the memory element.

In order to reduce the complexity of solving (3), we integrate directly (1) on both sides and then the 3D equations can be obtained:

$$\begin{aligned} L_1 \frac{dq_1}{dt} &= (q_1 + q_2) R_0 - \varphi_m - q_1 R_1, \\ L_2 \frac{dq_2}{dt} &= (q_1 + q_2) R_0 - \varphi_m - q_2 R_2, \\ \frac{d\sigma_m}{dt} &= q_1 + q_2 + q_0, \end{aligned} \tag{11}$$

where q_0 is the initial charge of the memcapacitor and q_1, q_2, φ_m, and σ_m are the time integrals of i_1, i_2, v_m, and q_m, respectively.

For convenience, let $x = q_1$, $y = q_2$, $z = \sigma_m$, $a = a/L_1$, $b = \beta/L_1$, $c = (R_0 - R_1)/L_1$, $d = R_0/L_1$, $e = (R_0 - R_2)/L_2$, $f = R_0/L_2$, $m = \beta/L_2$, $n = \alpha/L_2$, and $q_0 = 0$; (11) can be transformed as follows:

$$\begin{aligned} \frac{dx}{dt} &= cx + dy - az - bz^3, \\ \frac{dy}{dt} &= fx + ey - nz - mz^3, \\ \frac{dz}{dt} &= x + y. \end{aligned} \tag{12}$$

We now present the attracting basins shown in Figure 9 in the $x(0)$-$y(0)$ plane and the $x(0)$-$z(0)$ plane for observing the dynamics of the memcapacitor-based circuit. Here, we fix $a = 6.6$, $b = 1$, $c = 2.5$, $d = 0.25$, $e = -3.41$, $f = 0.25$, $m = 5.2$,

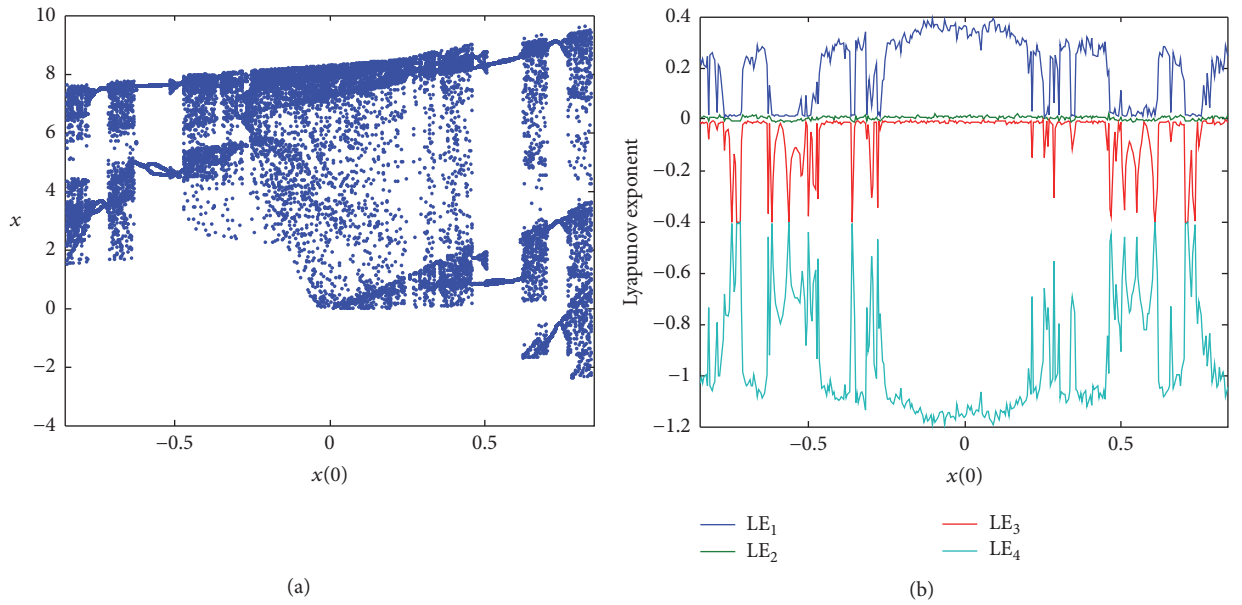

FIGURE 5: Bifurcation diagram and Lyapunov exponent spectrum of coexisting oscillation with respect to initial value $x(0)$. (a) Bifurcation diagram. (b) Lyapunov exponent spectrum.

TABLE 2: Coexisting attractors for various conditions $(x(0), 0.01, 0.01, 0)$.

Regimes	$x(0)$	Diagrams
A symmetric pair of chaotic attractors	−0.800	Figure 6(a), blue
	0.800	Figure 6(a), red
A symmetric pair of quasiperiodic limit cycles	−0.779	Figure 6(b), blue
	0.764	Figure 6(b), red
A symmetric pair of limit cycles	−0.490	Figure 6(c), blue
	0.470	Figure 6(c), red
A symmetric pair of chaotic attractors	−0.268	Figure 6(d), blue
	0.252	Figure 6(d), red
A symmetric pair of chaotic attractors	−0.250	Figure 6(e), blue
	0.190	Figure 6(e), red

and $n = 2$. And the initial conditions are $(x(0), y(0), 0.01)$ and $(x(0), 0.01, z(0))$ for Figures 9(a) and 9(b), respectively. Each attracting basin is divided into blue region and red region, corresponding to two types of coexisting attractors, which are shown in Figure 10.

The initial charge q_0 of the memcapacitor plays an important role in the circuit. The bifurcation diagram and corresponding Lyapunov exponent spectrum with respect to q_0 are presented in Figure 11 with the initial condition (0.01, 0.01, 0.01) and the parameters $a = 6.6, b = 1, c = 2.5, d = 0.25$, $e = -3.41$, $f = 0.25$, $m = 5.2$, and $n = 2$.

Figure 11(a) shows a complex bifurcation process, which has typical period 3 window, and also possesses novel period 1 and period 2 windows. Furthermore, there exist period-doubling and inverse period-doubling bifurcations in both sides of the period 2 window. Figures 12(a)–12(d) give the typical attractors in the y-z plane with $q_0 = 0.01$, $q_0 = 0.05$, $q_0 = 0.11$, and $q_0 = 0.29$.

5. Analog Circuit Experiment

An experimental circuit is designed to realize the memcapacitor-based chaotic oscillator. The designed circuit for realizing (12) is shown in Figure 13, and its corresponding state equations are written as

$$\begin{aligned}
\frac{dx}{d\tau} &= -\frac{1}{R_1C_1}(-x) - \frac{1}{R_2C_1}(-y) - \frac{1}{R_3C_1}z \\
&\quad - \frac{1}{100R_4C_1}z^3, \\
\frac{dy}{d\tau} &= -\frac{1}{R_5C_2}(-x) - \frac{1}{R_6C_2}y - \frac{1}{R_7C_2}z - \frac{1}{100R_8C_2}z^3, \\
\frac{dz}{d\tau} &= -\frac{1}{R_9C_3}(-x) - \frac{1}{R_{10}C_3}(-y).
\end{aligned} \tag{13}$$

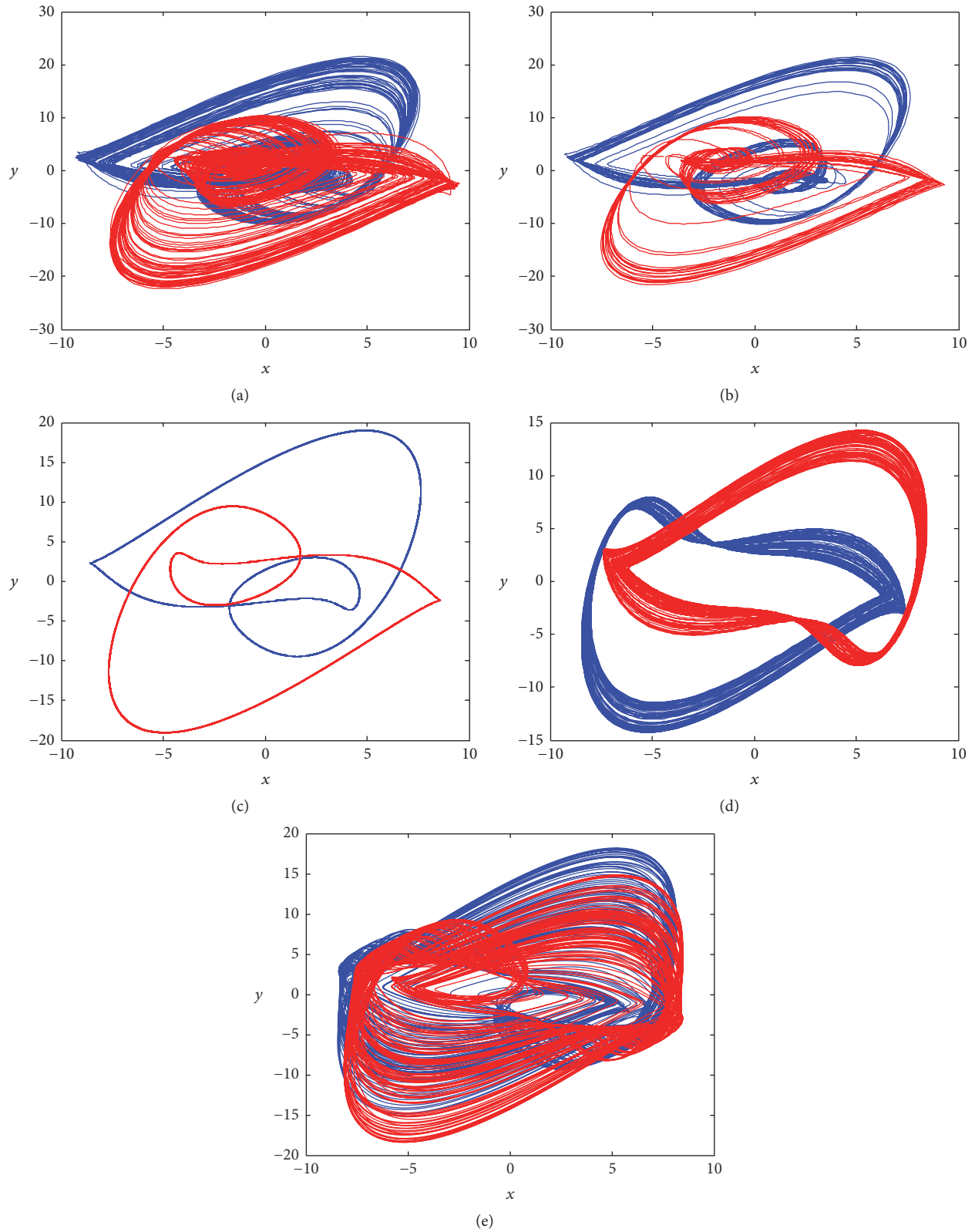

Figure 6: Coexisting attractors on x-y plane. (a) Coexistence of a symmetric pair of chaotic attractors with $x(0) = -0.800$ and $x(0) = 0.800$. (b) Coexistence of a symmetric pair of quasiperiodic limit cycles with $x(0) = -0.779$ and $x(0) = 0.764$. (c) Coexistence of a symmetric pair of limit cycles with $x(0) = -0.490$ and $x(0) = 0.470$. (d) Coexistence of a symmetric pair of chaotic attractors with $x(0) = -0.268$ and $x(0) = 0.252$. (e) Coexistence of a symmetric pair of chaotic attractors with $x(0) = -0.250$ and $x(0) = 0.190$.

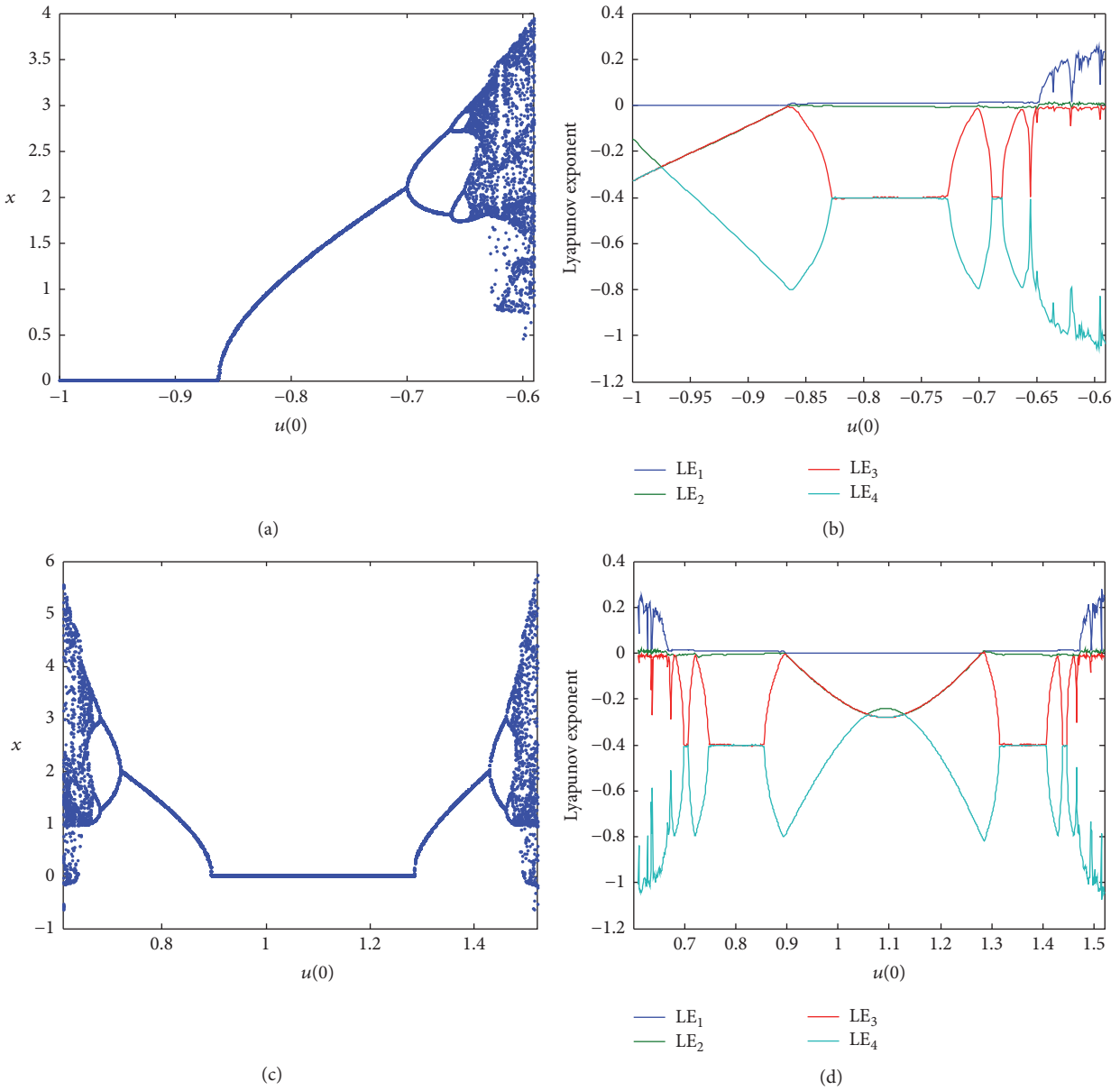

Figure 7: Bifurcation and Lyapunov exponents of coexisting oscillation with respect to initial $u(0)$. ((a) and (b)) Bifurcation diagrams. ((c) and (d)) Corresponding Lyapunov exponent spectrum.

Table 3: Coexisting attractors for initial condition $(0.01, 0.01, 0.01, u(0))$.

Regimes	$u(0)$	Diagrams
Point attractor	−0.865 and 0.865	Figure 8(a), black
A symmetric pair of limit cycles	−0.740	Figure 8(a), blue
	0.760	Figure 8(a), red
A symmetric pair of quasiperiodic limit cycles	−0.650	Figure 8(b), blue
	0.667	Figure 8(b), red
A symmetric pair of chaotic attractors	−0.635	Figure 8(c), blue
	0.650	Figure 8(c), red
A symmetric pair of chaotic attractors	−0.610	Figure 8(d), blue
	0.630	Figure 8(d), red

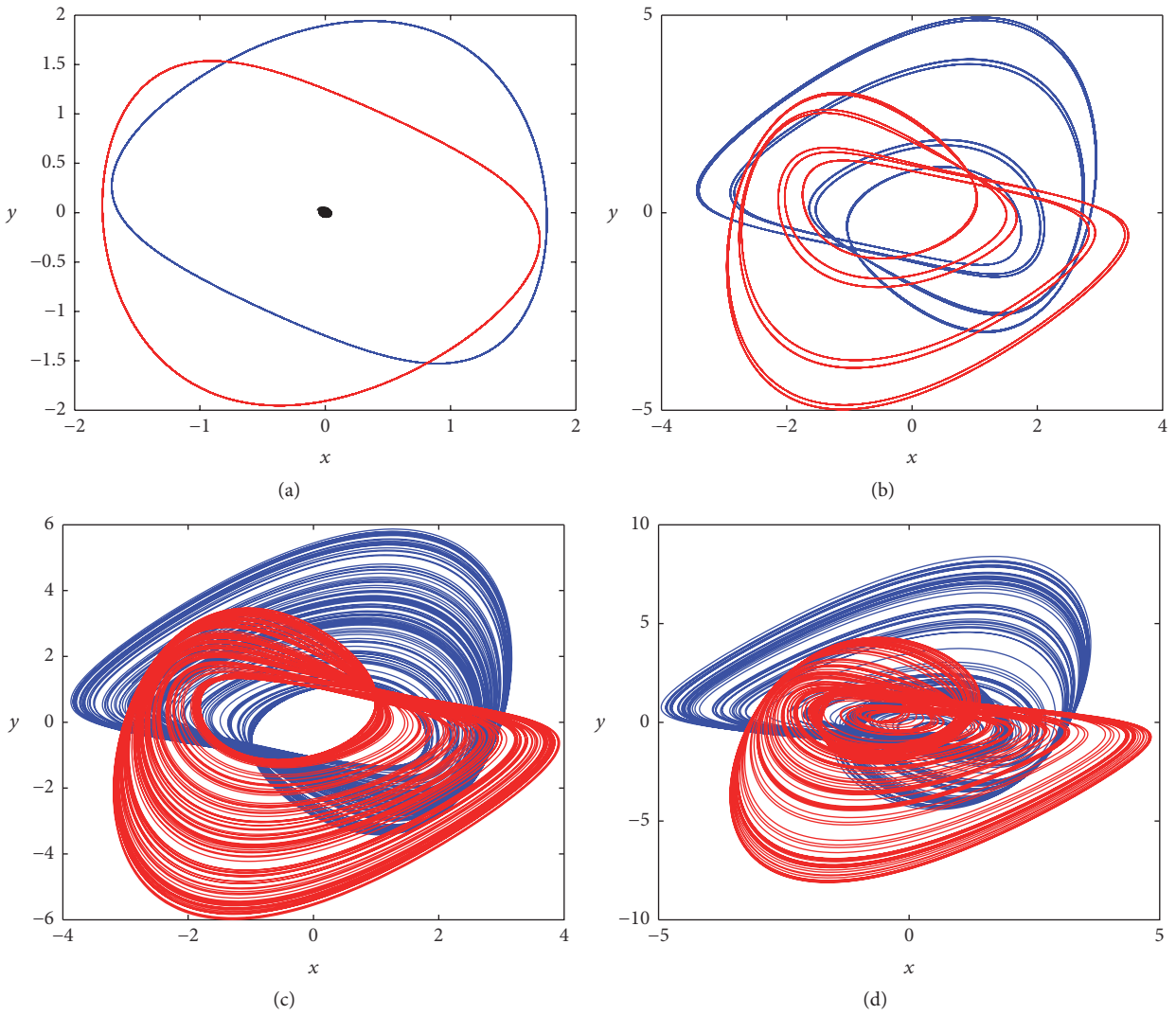

Figure 8: Coexisting attractors in the x-y plane with respect to $u(0)$. (a) Coexistence of a point attractor and a symmetric pair of limit cycles with $u(0) = -0.865$ (black), $u(0) = -0.740$ (blue), and $u(0) = 0.760$ (red), respectively. (b) Coexistence of a symmetric pair of quasiperiodic limit cycles with $u(0) = -0.650$ (blue) and $u(0) = 0.667$ (red). (c) Coexistence of a symmetric pair of chaotic attractors with $u(0) = -0.635$ (blue) and $u(0) = 0.650$ (red). (d) Coexistence of a symmetric pair of chaotic attractors with $u(0) = -0.610$ (blue) and $u(0) = 0.630$ (red).

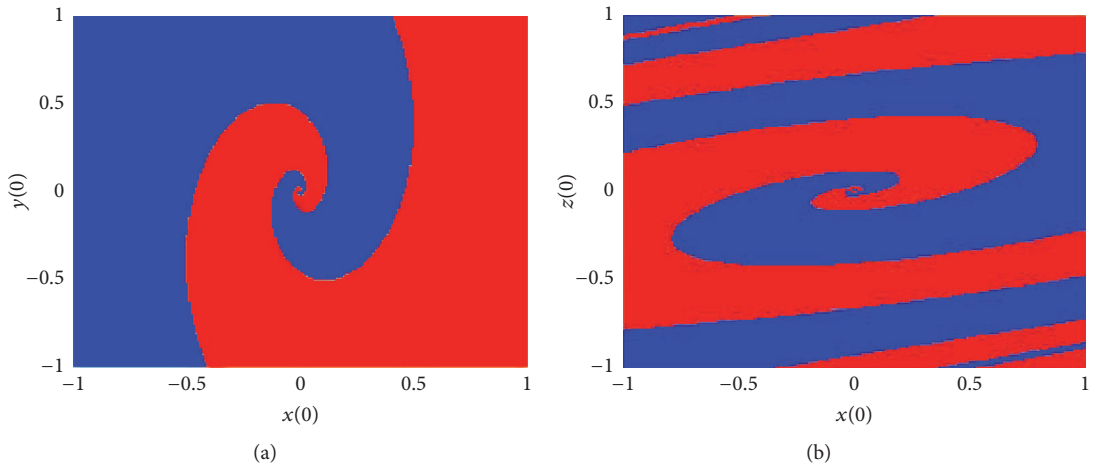

Figure 9: Cross sections of attracting basins for two chaotic attractors (blue and red). (a) $x(0)$-$y(0)$ plane. (b) $x(0)$-$z(0)$ plane.

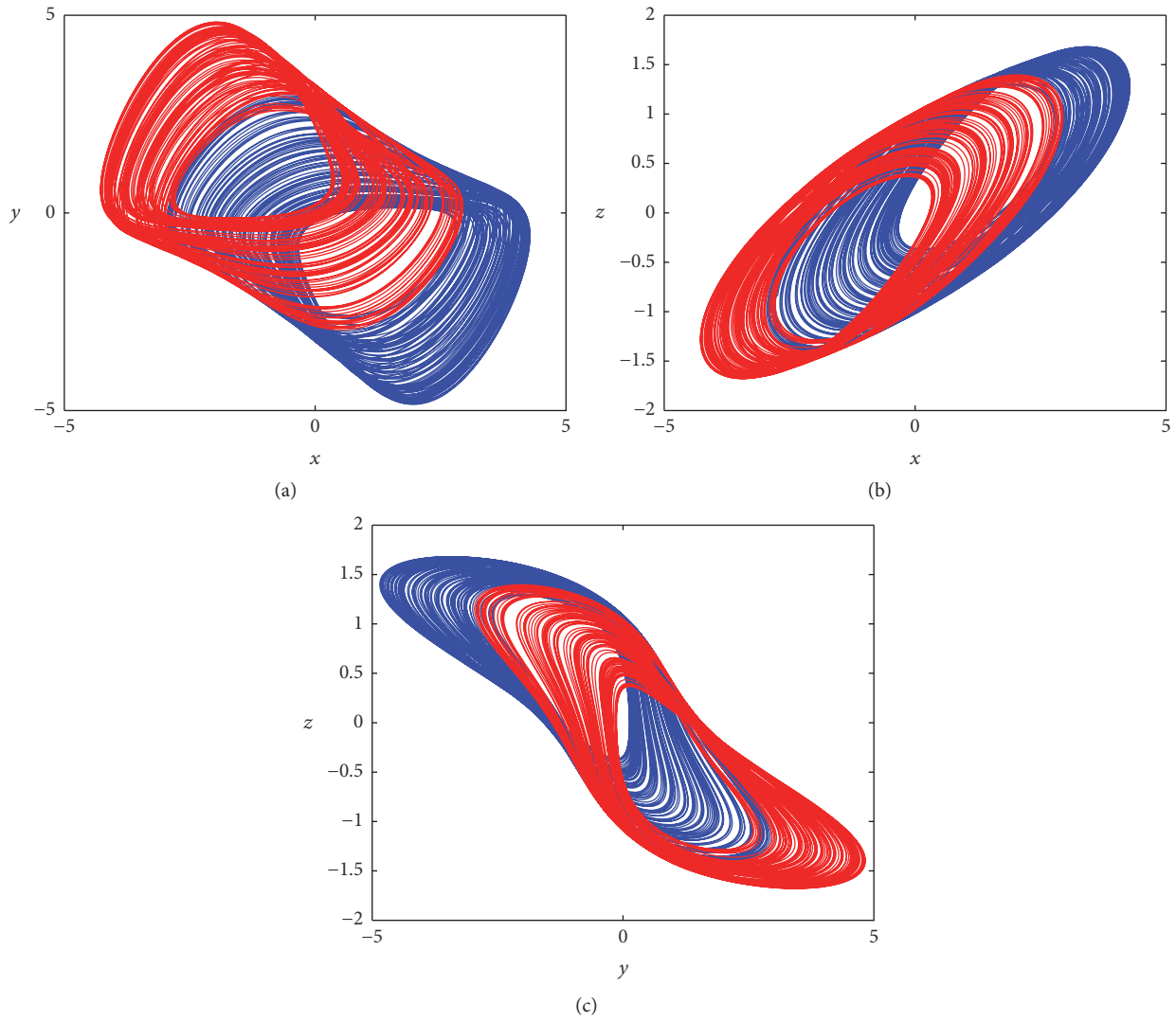

FIGURE 10: Coexisting chaotic attractors with initial conditions (0.01, 0.01, 0.01) (blue) and (0.01, 0.01, −0.01) (red). (a) x-y plane, (b) x-z plane cycles, and (c) y-z plane.

Circuit parameters can be obtained as $R_1 = 40\,\text{k}\Omega$, $R_2 = 400\,\text{k}\Omega$, $R_3 = 15\,\text{k}\Omega$, $R_4 = 1\,\text{k}\Omega$, $R_5 = 400\,\text{k}\Omega$, $R_6 \approx 30\,\text{k}\Omega$, $R_7 = 50\,\text{k}\Omega$, $R_8 \approx 180\,\Omega$, and $R_9 = R_{10} = 100\,\text{k}\Omega$, when we set $C_1 = C_2 = C_3 = C_4 = 10\,\text{nF}$, and $R_{11} = R_{12} = R_{13} = R_{14} = 100\,\text{k}\Omega$. In this circuit, the operational amplifier and the analog multiplier are selected as LF347N and AD633, respectively. The voltage references are ±VCC = ±15 V. The experimental chaotic attractors observed via the digital oscilloscope (DSO3102A) are shown in Figure 14.

Note that the circuit shown in Figure 13 and used in the experiment is designed based on (12), which is a set of dimension reduction (three-dimensional) equations which is obtained from five-dimensional equation (3). Compared with other memcapacitor-based chaotic oscillators, the advantages of this experiment are that the experimental circuit is simple and the attractors or time-domain waveforms with respect to charge (q_1 and q_2) through the inductor (L_1 and L_2) can be observed directly from the experimental oscilloscope.

6. Conclusion

In this paper, a new chaotic oscillator based on charge-controlled memcapacitor is designed. The dynamical characteristics with respect to the variations of initial conditions are investigated, and then the complex dynamic characteristics, including equilibrium set or an infinite number of equilibrium points, extreme multistability of the equilibrium set, and coexisting attractors, are found. Finally, chaotic attractors are captured experimentally by the analog circuit of implementing this oscillator. The most prominent feature of this system is the coexisting oscillation and coexisting attractors. It is concluded that one coexisting oscillation system can be as multi-random signal seeds to design different chaotic pseudorandom number generators, which can be used in secret communications, information encryptions, and various pseudorandom number generation.

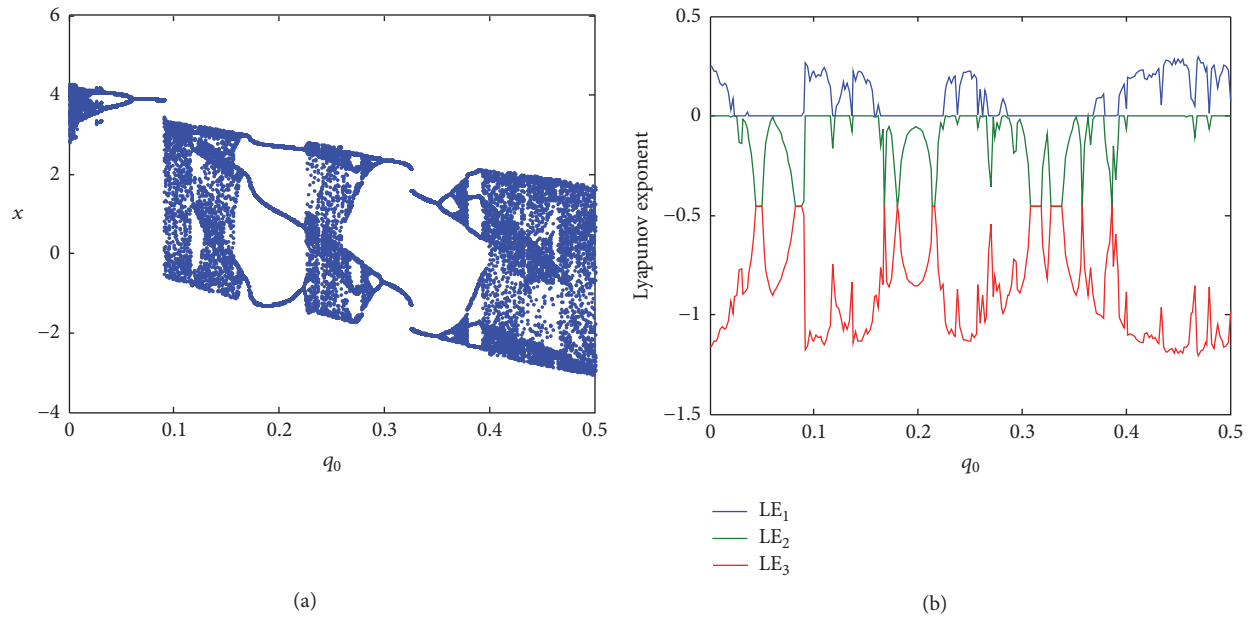

FIGURE 11: Bifurcation Lyapunov exponents with respect to q_0. (a) Bifurcation diagram. (b) Lyapunov exponent spectrum.

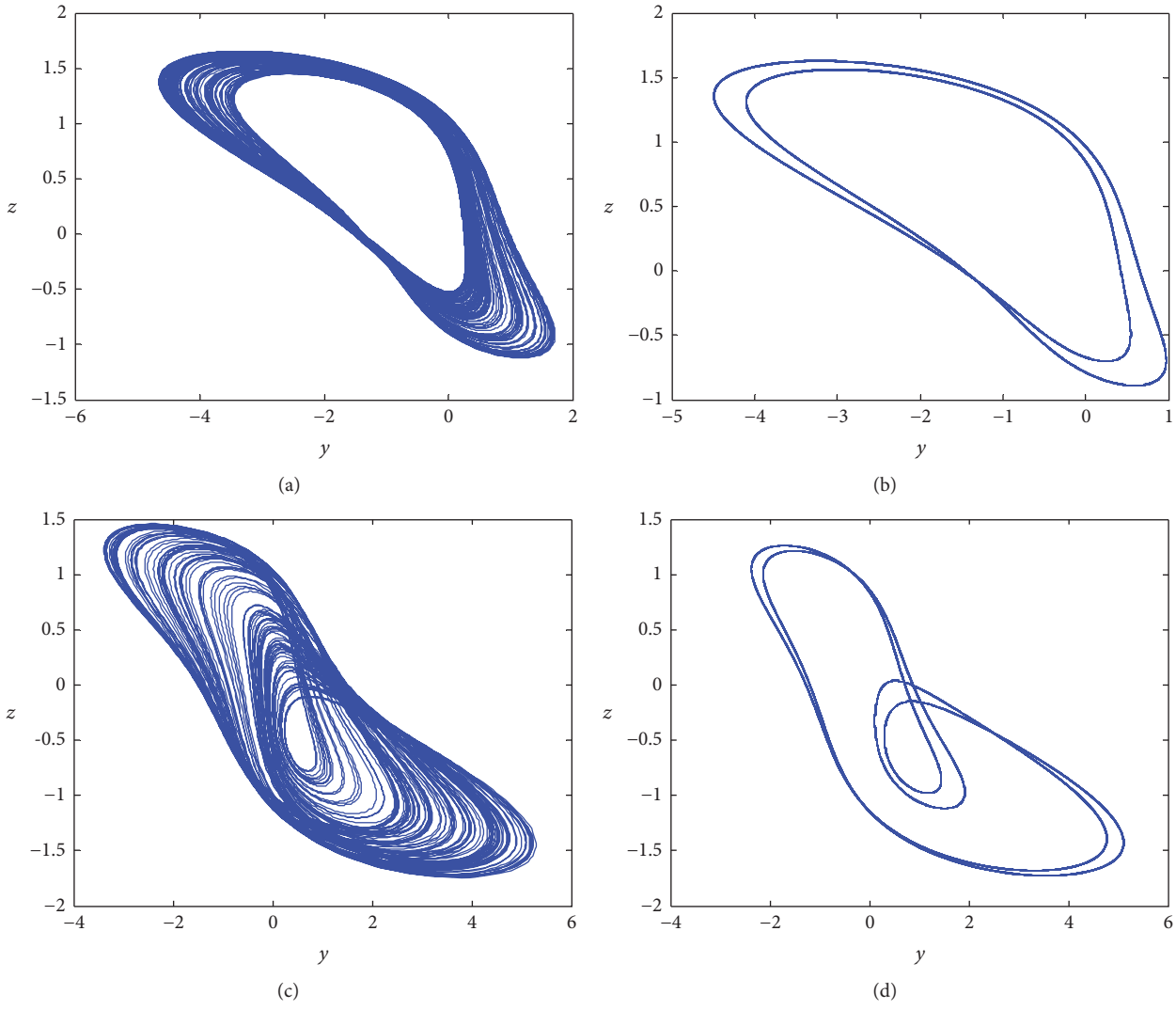

FIGURE 12: Evolved attractors in the y-z plane with respect to q_0. (a) Chaotic attractor with $q_0 = 0.01$. (b) Period 2 attractor with $q_0 = 0.05$. (c) Chaotic attractor with $q_0 = 0.11$. (d) Period 2 attractor with $q_0 = 0.29$.

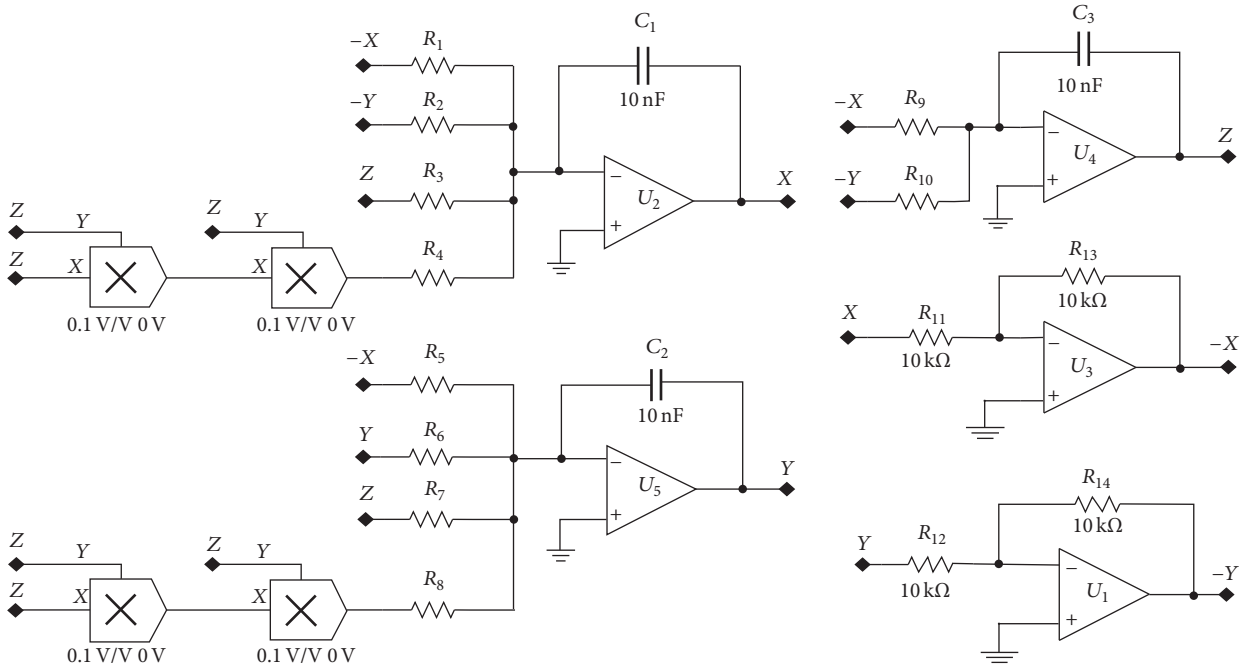

Figure 13: Circuit diagram of implementing (3).

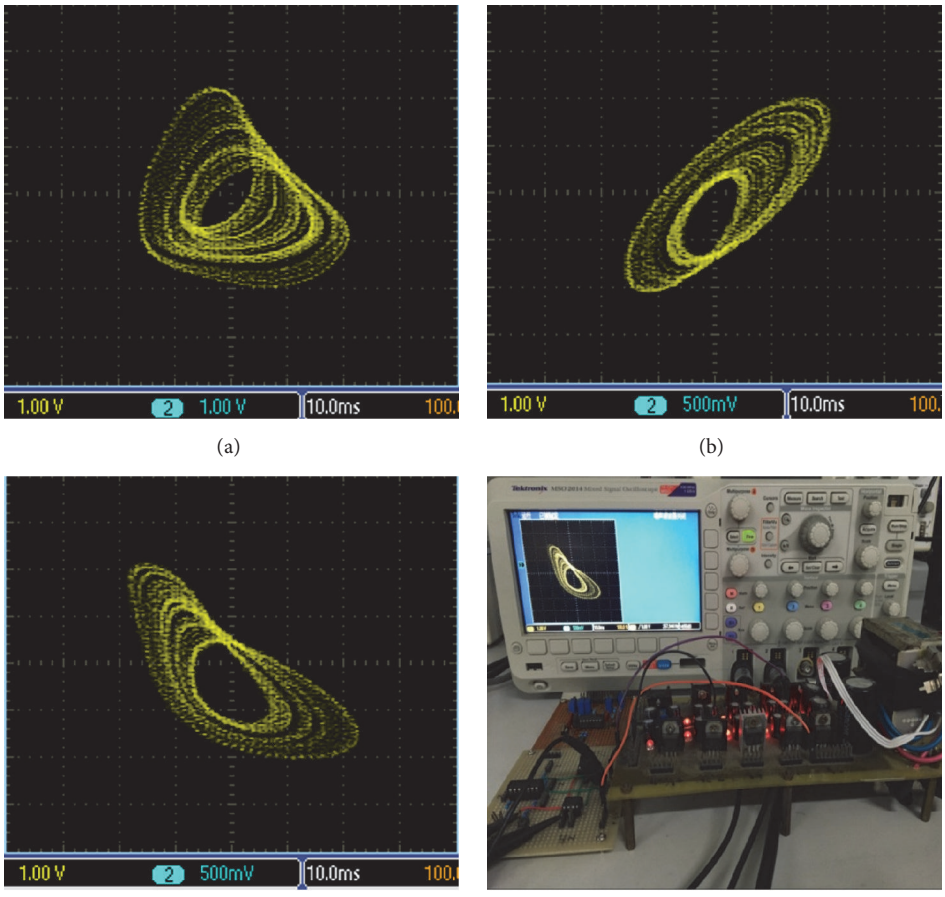

(a) (b)

(c) (d)

Figure 14: Experimental attractors and setup. (a) x-y plane. (b) x-z plane. (c) y-z plane. (d) Experimental setup.

Competing Interests

The authors declare that there is no conflict of interests regarding the publication of this paper.

Acknowledgments

This work was supported by the National Natural Science Foundation of China under Grant nos. 61271064 and 60971046 and the Program for Zhejiang Leading Team of S&T Innovation under Grant no. 2010R50010.

References

[1] L. O. Chua, "Memristorthe—missing circuit element," *IEEE Transactions on Circuit Theory*, vol. 18, no. 5, pp. 507–519, 1971.

[2] D. B. Strukov, G. S. Snider, D. R. Stewart, and R. S. Williams, "The missing memristor found," *Nature*, vol. 453, pp. 80–83, 2008.

[3] M. Di Ventra, Y. V. Pershin, and L. O. Chua, "Circuit elements with memory: memristors, memcapacitors, and meminductors," *Proceedings of the IEEE*, vol. 97, no. 10, pp. 1717–1724, 2009.

[4] M. Itoh and L. O. Chua, "Memristor oscillators," *International Journal of Bifurcation and Chaos*, vol. 18, no. 11, pp. 3183–3206, 2008.

[5] H. Kim, M. P. Sah, C. Yang, S. Cho, and L. O. Chua, "Memristor emulator for memristor circuit applications," *IEEE Transactions on Circuits and Systems I: Regular Papers*, vol. 59, no. 10, pp. 2422–2431, 2012.

[6] B. Bao, P. Jiang, H. Wu, and F. Hu, "Complex transient dynamics in periodically forced memristive Chua's circuit," *Nonlinear Dynamics*, vol. 79, no. 4, pp. 2333–2343, 2015.

[7] L. Wang, E. Drakakis, S. Duan, P. He, and X. Liao, "Memristor model and its application for chaos generation," *International Journal of Bifurcation and Chaos*, vol. 22, no. 8, Article ID 1250205, 2012.

[8] M. Itoh and L. O. Chua, "Dynamics of memristor circuits," *International Journal of Bifurcation and Chaos*, vol. 24, no. 5, Article ID 1430015, 44 pages, 2014.

[9] G. Wang, M. Cui, B. Cai, X. Wang, and T. Hu, "A chaotic oscillator based on HP memristor model," *Mathematical Problems in Engineering*, vol. 2015, Article ID 561901, 12 pages, 2015.

[10] F. Yuan, G.-Y. Wang, and X.-Y. Wang, "Dynamical characteristics of an HP memristor based on an equivalent circuit model in a chaotic oscillator," *Chinese Physics B*, vol. 24, no. 6, Article ID 060506, 2015.

[11] Y.-M. Xu, L.-D. Wang, and S.-K. Duan, "A memristor-based chaotic system and its field programmable gate array implementation," *Acta Physica Sinica*, vol. 65, no. 12, Article ID 120503, 2016.

[12] Z. S. Yuan, H. T. Li, and X. H. Zhu, "A digital-analog hybrid random number generator based on memristor," *Acta Physica Sinica*, vol. 64, no. 24, Article ID 0240503, 2015.

[13] J. Han, C. Song, S. Gao, Y. Wang, C. Chen, and F. Pan, "Realization of the meminductor," *ACS Nano*, vol. 8, no. 10, pp. 10043–10047, 2014.

[14] F. Yuan, G. Wang, P. Jin, X. Wang, and G. Ma, "Chaos in a meminductor-based circuit," *International Journal of Bifurcation and Chaos in Applied Sciences and Engineering*, vol. 26, no. 8, Article ID 1650130, 14 pages, 2016.

[15] Y. Liang, D.-S. Yu, and H. Chen, "A novel meminductor emulator based on analog circuits," *Acta Physica Sinica*, vol. 62, no. 15, Article ID 158501, 2013.

[16] G. Wang, P. Jin, X. Wang, Y. Shen, F. Yuan, and X. Wang, "A flux-controlled model of meminductor and its application in chaotic oscillator," *Chinese Physics B*, vol. 25, no. 9, p. 090502, 2016.

[17] Y. V. Pershin and M. Di Ventra, "Emulation of floating memcapacitors and meminductors using current conveyors," *Electronics Letters*, vol. 47, no. 4, pp. 243–244, 2011.

[18] D. S. Yu, Y. Liang, H. Chen, and H. H. C. Iu, "Design of a practical memcapacitor emulator without grounded restriction," *IEEE Transactions on Circuits and Systems II: Express Briefs*, vol. 60, no. 4, pp. 207–211, 2013.

[19] A. L. Fitch, H. H. C. Iu, and D. S. Yu, "Chaos in a memcapacitor based circuit," in *Proceedings of the IEEE International Symposium on Circuits and Systems (ISCAS '14)*, pp. 482–485, IEEE, Sydney, Australia, June 2014.

[20] D. Biolek, Z. Biolek, and V. Biolková, "Behavioral modeling of memcapacitor," *Radioengineering*, vol. 20, no. 1, pp. 228–233, 2011.

[21] X. Y. Wang, A. L. Fitch, H. H. C. Iu, and W. G. Qi, "Design of a memcapacitor emulator based on a memristor," *Physics Letters A*, vol. 376, no. 4, pp. 394–399, 2012.

[22] M. E. Fouda and A. G. Radwan, "Charge controlled memristor-less memcapacitor emulator," *Electronics Letters*, vol. 48, no. 23, pp. 1454–1455, 2012.

[23] G.-Y. Wang, B.-Z. Cai, P.-P. Jin, and T.-L. Hu, "Memcapacitor model and its application in a chaotic oscillator," *Chinese Physics B*, vol. 25, no. 1, Article ID 010503, 2015.

[24] F. Yuan, G. Wang, Y. Shen, and X. Wang, "Coexisting attractors in a memcapacitor-based chaotic oscillator," *Nonlinear Dynamics*, vol. 86, no. 1, pp. 37–50, 2016.

[25] M. E. Fouda and A. G. Radwan, "Resistive-less memcapacitor-based relaxation oscillator," *International Journal of Circuit Theory and Applications*, vol. 43, no. 7, pp. 959–965, 2015.

[26] F. Yuan, G. Wang, and X. Wang, "Extreme multistability in a memristor-based multi-scroll hyper-chaotic system," *Chaos*, vol. 26, no. 7, Article ID 073107, 2016.

[27] M. Chen, M. Y. Li, Q. Yu, B. Bao, Q. Xu, and J. Wang, "Dynamics of self-excited attractors and hidden attractors in generalized memristor-based Chua's circuit," *Nonlinear Dynamics*, vol. 81, no. 1-2, pp. 215–226, 2015.

[28] J. Kengne, Z. N. Tabekoueng, V. K. Tamba, and A. N. Negou, "Periodicity, chaos, and multiple attractors in a memristor-based Shinriki's circuit," *Chaos*, vol. 25, no. 10, Article ID 103126, 10 pages, 2015.

[29] C. Li and J. C. Sprott, "Multistability in a butterfly flow," *International Journal of Bifurcation and Chaos in Applied Sciences and Engineering*, vol. 23, no. 12, Article ID 1350199, 2013.

[30] C. Li and J. C. Sprott, "Coexisting hidden attractors in a 4-D simplified Lorenz system," *International Journal of Bifurcation and Chaos*, vol. 24, no. 3, Article ID 1450034, 12 pages, 2014.

[31] U. Feudel, "Complex dynamics in multistable systems," *International Journal of Bifurcation and Chaos*, vol. 18, no. 6, pp. 1607–1626, 2008.

[32] C. N. Ngonghala, U. Feudel, and K. Showalter, "Extreme multistability in a chemical model system," *Physical Review E—Statistical, Nonlinear, and Soft Matter Physics*, vol. 83, no. 5, Article ID 056206, 2011.